Anal Bioanal Chem (2006) 385: 678–685
DOI 10.1007/s00216-006-0453-y

ORIGINAL PAPER

Kyle W. Kimble · Jeremy P. Walker ·
David N. Finegold · Sanford A. Asher

Progress toward the development of a point-of-care photonic crystal ammonia sensor

Received: 26 January 2006 / Revised: 27 March 2006 / Accepted: 28 March 2006 / Published online: 5 May 2006

Abstract We have developed an ammonia-sensitive material by coupling the Berthelot reaction to our polymerized crystalline colloidal array (PCCA) technology. The material consists of a periodic array of highly charged colloidal particles (110 nm diameter) embedded in a poly(hydroxyethyl acrylate) hydrogel. The particles have a lattice spacing such that they Bragg-diffract visible light. In the Berthelot reaction, ammonia, hypochlorite, and phenol react to produce the dye molecule indophenol blue in an aqueous solution. We use this reaction in our sensor by covalently attaching 3-aminophenol to the hydrogel backbone, which forms cross-links through the Berthelot mechanism. Ammonia reacts with hypochlorite, forming monochloramine, which then reacts with a pendant aminophenol to form a benzoquinone chlorimine. The benzoquinone chlorimine reacts with another pendant aminophenol to form a cross-link. The creation of new cross-links causes the hydrogel to shrink, which reduces the lattice spacing of the embedded colloidal array. This volume change results in a blue-shift in the diffracted light proportional to the concentration of NH_3 in the sample. We demonstrate that the NH_3 photonic crystal sensing material is capable of quantitative determination of concentrations in the physiological range (50–350 μmol NH_3 L^{-1}) in human blood serum.

Keywords Sensor · Ammonia · Point-of-care · Polymerized crystalline colloidal array (PCCA) · Hydrogels · Photonic crystal

K. W. Kimble · J. P. Walker · D. N. Finegold · S. A. Asher (✉)
Department of Chemistry, School of Medicine,
Chevron Science Center, University of Pittsburgh,
Pittsburgh, PA 15260, USA
e-mail: asher@pitt.edu
Tel.: +1-412-6248570
Fax: +1-412-6240588

Introduction

Ammonia within bodily fluids results from metabolic breakdown of dietary proteins and is generated primarily in the liver, muscles, and kidneys [1]. It arises specifically from deamination of the α-amino nitrogen of amino acids and is toxic when persistent at elevated levels. Hyperammonemia, venous blood levels of ammonia greater than 100 μmol NH_3 L^{-1} in neonates, or greater than 40 μmol NH_3 L^{-1} in others, results primarily from one of four groups of diagnoses: urea cycle disorders (UCDs), organic acidemias (OAs), fatty acid oxidation defects (FAOs), and liver malfunction [2, 3].

Hyperammonemia results in damage to the central nervous system, including alteration of the transit of amino acids, water, and electrolytes across the neuronal membrane. Ammonia can also inhibit the generation of both excitatory and inhibitory postsynaptic potentials [4, 5]. Routine screening of ammonia levels would enable treatment of at-risk patients before hyperammonemia caused retardation, neurological damage, or death. The frequency of testing required to avoid the physical ramifications of hyperammonemia places a high demand both on clinical laboratories and on affected patients and families [6].

Blood ammonia levels are currently determined by using an enzyme-based assay in which the enzyme glutamate dehydrogenase converts 2-oxoglutarate and ammonium to glutamate and water. In this reaction, the UV absorbance of the NADPH cofactor is monitored as it is converted to $NADP^+$ [2, 7–9]. This test requires sophisticated laboratory instrumentation and testing is typically performed in clinical laboratories. Further complicating ammonia determinations, whole blood samples begin to generate ammonia immediately after being taken, because of deamination of proteins in the red blood cells (RBCs). Blood from a healthy person can be stored at 4 °C for an hour, but patients with urea cycle defects must have their blood analyzed or treated within 15–30 min of sampling if accurate results are to be obtained. This need for immediate testing is a substantial obstacle to the accurate determination

of ammonia and requires that the patient be tested in close proximity to the clinical laboratory [10].

Numerous other techniques have been developed for detection of ammonia in body fluids. Unlike the direct enzymatic method mentioned above, most of these are two-step processes. The first step separates ammonia from the biological matrix; the second step is a quantitative determination. Means of separation of ammonia from the blood include distillation, aeration, ion-exchange, microdiffusion, protein precipitation, or Kjeldahl extraction [11–14]. Several methods have been developed which are based on the alkaline liberation of gaseous ammonia and transport through a gas-permeable membrane. Subsequent determination of the ammonia is performed by colorimetry, titration, ion-selective electrochemistry, fluorimetry, conductometry, mass spectrometry, second-derivative spectrometry, optical waveguide spectroscopy, HPLC, or capillary isotachophoresis [15]. Several techniques have also been developed which combine liberation and quantitation in one procedure. These techniques were discussed at length in the recent review by Huizenga et al. [10].

A colorimetric approach to sensing ammonia which has been successful in solution is the Berthelot, or indophenol, reaction [16]. In this reaction, ammonia (NH_3) reacts with a hypochlorite (OCl^-) to form a monochloramine, which in turn reacts with two phenols to form an indophenol dye (Fig. 1). The concentration of NH_3 can be determined by monitoring the absorbance of the dye molecule at λ=640 nm. This reaction has been extensively studied in solution for a variety of absorbing phenolic species and hypohalite sources [17]. A variety of catalysts have also been explored as a means of increasing reaction kinetics. The most prevalently used catalyst is sodium nitroferricyanide(III) dihydrate (nitroprusside, NP). Several researchers have effectively demonstrated the coupling of alkaline liberation of NH_3 with the Berthelot determination [10].

The Berthelot reaction has some drawbacks. The change in absorbance resulting from the Berthelot reaction cannot be monitored visually, because physiological concentrations of NH_3 result in small indophenol absorbance changes. Not only does this require the use of a spectrophotometer to measure these subtle changes, but the indophenol molecule is also subject to photodegradation. The Berthelot method is also known to suffer from interferences from other amine-containing molecules present in the analyte matrix [18, 19].

Building on the concept of home glucose monitoring we have attempted to design a sensing material that can be incorporated into new technology for home or bed-side point-of-care NH_3 monitoring. To accomplish this, the sensor must be inexpensive, reproducible, and robust. It must also be chemically sensitive, accurate, and capable of sensing very small volumes of capillary blood (20 μL). Finally, it must display information in a format that is easily interpreted.

Our NH_3 sensor is based on our previously developed PCCA photonic crystal sensing technology (Fig. 2) [20–33]. Our PCCAs utilize an array of highly charged colloidal particles embedded in a hydrogel matrix. The array of particles Bragg-diffracts light in the visible region of the spectrum. Our molecular recognition agent, 3-aminophenol, is covalently attached to the hydrogel. The OCl^- and NH_3 react in the test solution to form monochloramine, which in turn reacts with two of the pendant 3-aminophenols to create a new cross-link in the hydrogel. The formation of cross-links in the hydrogel matrix increases the elastic restoring force of the hydrogel network and actuates an osmotic

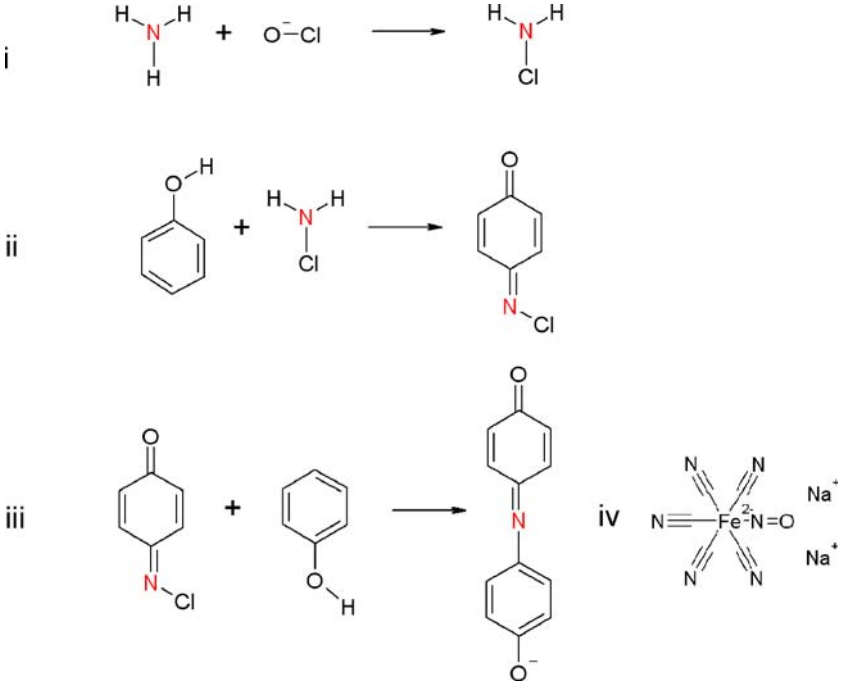

Fig. 1 The reaction mechanism proposed for the Berthelot reaction consists of three steps: (*i*) ammonia reacts with hypochlorite to form monochloramine at basic pH, (*ii*) monochloramine reacts with a phenol to form benzoquinone chlorimine, (*iii*) benzoquinone chlorimine reacts with a second phenol to form an indophenol. (*iv*) Sodium nitroferricyanide(III) dihydrate is a coupling reagent which increases the kinetics of step (*ii*)

pressure inside the gel which causes the hydrogel to shrink in proportion to the amount of NH_3 present in solution. This results in a decrease in the spacing between diffracting planes of the embedded colloidal array and a blue-shift in the wavelength of light diffracted by the sensor. Our NH_3 sensor relies on changes in the elastic free-energy of the hydrogel caused by the formation of cross-links. The diffraction blue-shift can be directly correlated with the amount of NH_3 present in the analyte solution. We have also recently improved our modeling of these PCCA sensing volume phase transitions [34].

The wavelength of light (λ_o) diffracted follows Bragg's law: $\lambda=2nd\sin\theta$. In our sensor the light is diffracted by the fcc 111 plane of the embedded particle array. λ depends on the plane spacing, d, the refractive index of the system, n, and the incident angle of the light, θ, which is the Bragg glancing angle. Because we are sampling back-diffraction (reflectance) from light normally incident to the 111 plane of the array, $\sin\theta$ is unity.

Experimental

PCCA preparation Figure 3 depicts the synthesis and functionalization of the PCCA. 2-hydroxyethyl acrylate (2-HEA, 0.94 g, 8.1 mmol; Sigma), poly(ethylene glycol) (200) dimethacrylate (PEGDMA-200, 0.09 g, 0.25 mmol; Polysciences), glycidyl acrylate (GA, 0.04 g, 0.37 mmol; Sigma), and ethylene glycol (1.95 g, 31 mmol; J.T. Baker) were mixed and treated with Al_2O_3 to remove the inhibitor from the monomers. The mixture was centrifuged to separate the monomer from the Al_2O_3. This solution (1.015 g) was mixed with the colloid suspension (1.0 g, 5–10 % *m*/*m* dispersion, polystyrene latex spheres, 110 nm). AG501-X8 (D) ion exchange resin (~0.1 g, 20–50 mesh, mixed bed; Bio-Rad), and 10 % diethoxyacetophenone (DEAP, 10 μL, 4 μmol; Aldrich) in DMSO (J.T. Baker) were mixed into the suspension in a 2-dr vial. After 15 min the mixture was centrifuged to remove the ion-exchange resin and was injected between two quartz discs separated by a 125-μm thick Parafilm spacer. The colloidal particles self-assemble into a crystalline colloidal array (CCA), resulting in a liquid film which diffracts light. The film was exposed to UV light (λ=365 nm) from mercury lamps (Blak Ray) for 3 h. A poly-HEA hydrogel network with PEGDMA cross-links forms around the CCA, resulting in a polymerized CCA (PCCA). The cell enclosing the hydrogel was opened in Nanopure water and the PCCA was left to equilibrate with water.

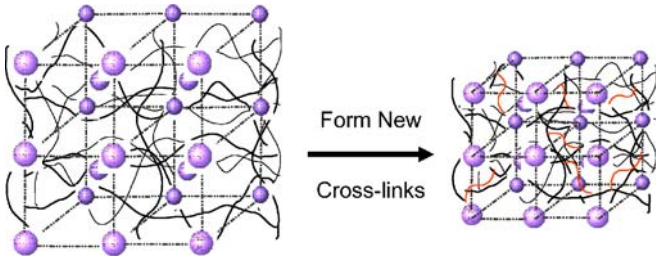

Fig. 2 The formation of indophenol cross-links results in an increase in the elastic restoring force of the hydrogel, which actuates an osmotic pressure, forcing water out of the hydrogel and thereby reducing the volume of the gel. As a result, the spacing between diffracting planes in the PCCA decreases, and the wavelength of diffracted light blue-shifts in proportion to NH_3 concentration

Attachment of 3-aminophenol The PCCA was placed in a 50 mmol L^{-1} borate buffer solution (BBS, pH 9.2; J.T. Baker) to equilibrate before coupling. 3-Aminophenol (3-AMP, 4.6 mmol, 0.5 g; Sigma) was dissolved in 10 mL DMSO (J.T. Baker) and then diluted to 50 mL with 50 mmol BBS L^{-1}. The solution and PCCA were placed in a 125-mL plastic container (Nalgene) and were left to react for ~8 h. After reacting, the PCCA was rinsed every hour for 6 h with BBS. A blank gel (hydrogel without colloid) was prepared and functionalized by the same procedure. UV–visible spectra of the blank gel were measured by means of a Varian Cary 5000 UV–visible spectrophotometer to confirm attachment of 3-AMP by monitoring absorbance at λ=290 nm.

Diffraction measurements The diffraction of the PCCA was monitored by using a fiber-optic diode spectrometer with a tungsten halogen light source (Ocean Optics) using a reflectance probe. The light is completely diffracted by the first 10–20 μm thickness of the PCCA, because of the high diffraction efficiency of the embedded CCA [24].

A PCCA (1 cm×1 cm×125 μm) was attached to a plastic Petri dish and was equilibrated with 5 mL 50 mmol BBS L^{-1} containing sodium nitroferricyanide(III) dihydrate (nitroprusside, NP, 0.0188 g, 0.0125 mol L^{-1}; Aldrich). A standard NH_3 solution was prepared by dissolving 0.03 g NH_4Cl (5.6 mmol; J.T. Baker) in BBS and diluting to a total volume of 30 mL. An NaOCl solution was prepared by diluting 2.4 mL NaOCl (5 % in H_2O, 1.8 μmol; J.T. Baker) in BBS to a total volume of 30 mL. An initial diffraction spectrum of the PCCA was collected, and then an aliquot of the stock NH_3 solution was added to each piece of PCCA. After leaving the NH_3 to equilibrate for 5 min, 28 μL OCl^- solution was added. The diffraction spectra were recorded at pre-selected 5-min time intervals for a total of 120 min. The process was performed for NH_3 concentrations of 30, 75, 150, and 300 μmol NH_3 L^{-1}, each solution contained 600 μmol NaOCl L^{-1}. In a control measurement, a PCCA with 3-AMP attached was exposed to 600 μmol NaOCl L^{-1} solution with no NH_3 present, and diffraction spectra were collected in accordance with the procedure described above.

The response of a PCCA, synthesized without GA or 3-AMP, was monitored to establish that the attached 3-AMP was responsible for the blue-shift observed. This PCCA was tested in 0 and 300 μmol NH_3 L^{-1} solutions containing 600 μmol NaOCl L^{-1}.

The response of the PCCA to NH_3 was also tested in a solution which was isotonic to physiological fluid (~150 mmol NaCl L^{-1}), to determine whether salinity affects the response of the sensor. The response of the sensor to 100, 200, and 300 μmol NH_3 L^{-1} was determined in accordance with the procedure described above for solutions containing 50 mmol BBS L^{-1} and 100 mmol NaCl L^{-1}.

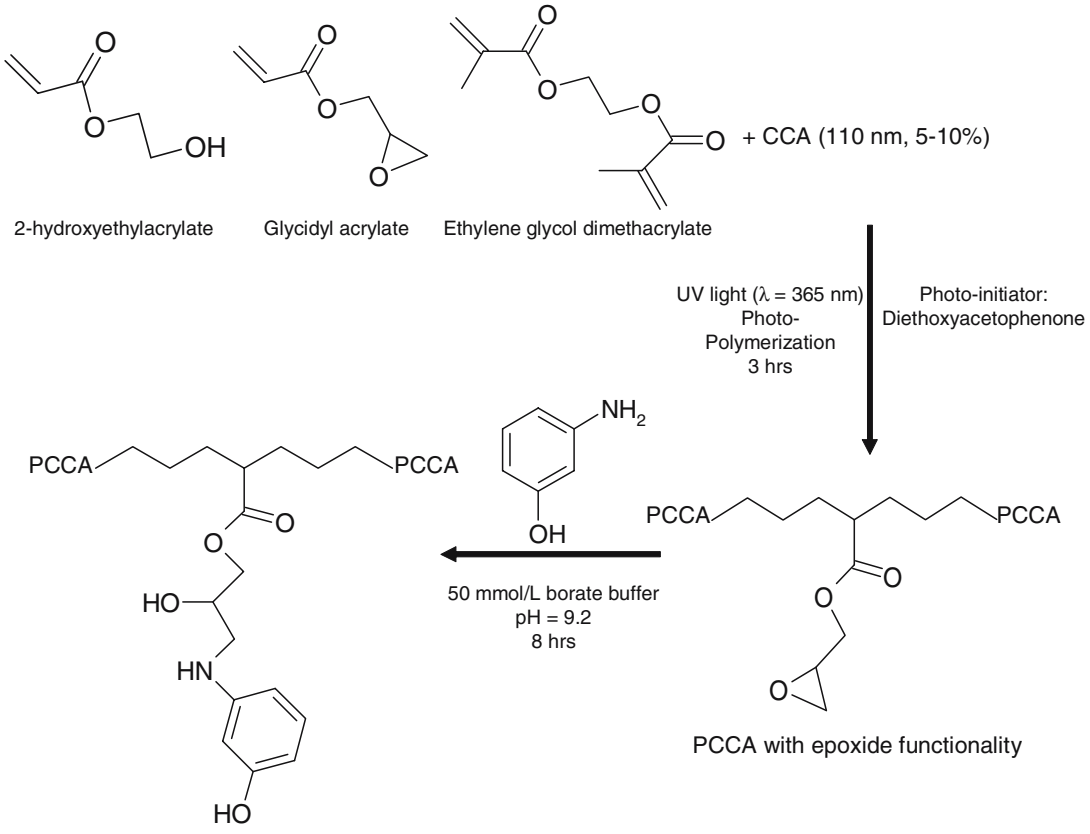

Fig. 3 Preparation and functionalization of PCCA by epoxide ring opening with 3-aminophenol

The sensor was tested in 5 mL of a 1:1 solution of BBS and male human serum from whole blood (Sigma). Mixing BBS (pH=9.2) with the serum resulted in a pH of 9.0. Four separate samples were spiked with concentrations of 30, 75, 150, and 300 μmol NH_3 L^{-1}. A fifth solution was not spiked, and was used to determine the spectral response generated from the NH_3 originally present in the sample. OCl^- was added to the solutions after equilibration (15 min), and diffraction spectra were recorded for 120 min. These five samples were also analyzed using a Vitros Chemistry Autoanalyzer System [9].

The sensor was tested in 5 mL solutions of BBS and bovine serum albumin (BSA, 35 mg mL^{-1} in BBS, Sigma). The response of the sensor to addition of OCl^- without NH_3 was determined.

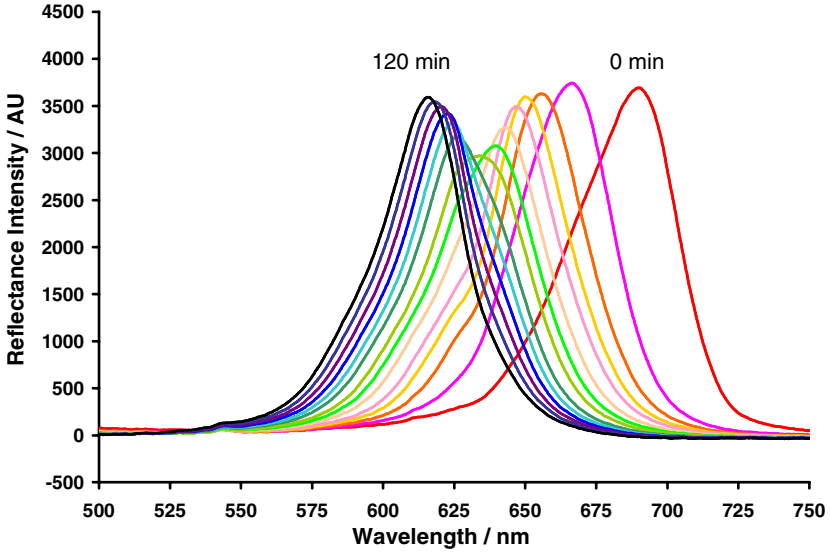

Fig. 4 Diffraction spectra of PCCA in the presence of 300 μmol NH_3 L^{-1}. The PCCA blue-shifts continuously over the course of 120 min as NH_3 reacts with OCl^- and 3-AMP to form an indophenol species which cross-links the hydrogel

Results and discussion

The normal physiological range of NH_3 in capillary blood is 19–54 μg NH_3 dL^{-1} (11–32 μmol NH_3 L^{-1}) according to Tietz [2] or 31–122 μg NH_3 dL^{-1} (18–72 μmol NH_3 L^{-1}) according to Pesce [3]. Neurological manifestations of elevated blood NH_3 are expected above 250 μg NH_3 dL^{-1} (147 μmol NH_3 L^{-1}) [3]. A sensor capable of determining the concentration of NH_3 from 10–300 μmol NH_3 L^{-1} in blood would be a valuable asset to the medical community.

Figure 4 shows the manner in which the diffraction spectrum (measured as reflectance) changes over time for 300 μmol NH_3 L^{-1} in BBS.

The longest-wavelength diffraction peak ($\lambda_{diffraction}$= 691 nm) corresponds to 0 min, directly after the addition of OCl^-. The shortest-wavelength diffraction peak ($\lambda_{diffraction}$=617 nm) corresponds to 120 min. The diffraction spectra shown were taken at 5 min intervals for the first 20 min and every 10 min thereafter. The sensor blue-shifts with time as the indophenol cross-links are formed. The change in the primary diffraction wavelength can be detected by a spectrometer, but it can also be observed visually.

Sensor response to NH_3 in buffer Figure 5 shows the diffraction blue-shift as a function of time for several concentrations of NH_3, and for a control with no NH_3 present. Each sample contained 600 μmol OCl^- L^{-1}. The rate of blue-shift was faster for higher concentrations of NH_3. All samples containing NH_3 result in diffraction blue-shifts. The control, which contains no NH_3, red-shifts.

The lack of blue-shift in the control indicates that no cross-links are formed without NH_3 present. The diffraction red-shift is presumably caused by hydrolysis of the poly(ethylene glycol) cross-linking esters at basic pH; this reduces the elastic restoring force of the PCCA and causes the hydrogel to expand. Because the red-shift is accelerated in the presence of OCl^-, we assume the OCl^- accelerates hydrolysis of the cross-link esters. Our hypothesis that the cross-link ester groups are being hydrolyzed is confirmed by observing an unfunctionalized PCCA (no GA or 3-AMP) swell on addition of OCl^-. The extent and rate of the red-shift was independent of the presence of 3-AMP. Figure 6 shows the NH_3 response calibration plots constructed from the observed shifts at 60 and 120 min in 50 mmol BBS L^{-1}. The plot has been corrected by subtracting the red-shift of the control from each spiked sample.

The response of the sensor is linear at 60 min for NH_3 concentrations between 30 and 150 μmol L^{-1}, but begins to saturate at NH_3 concentrations greater than 150 μmol L^{-1}. The response is curvelinear at longer times. The deviation from linearity presumably occurs because the concentrations of available OCl^- and 3-AMP are depleted as the reaction proceeds. This effect is exacerbated after longer times and higher NH_3 concentrations. At low concentrations of NH_3 the 3-AMP and OCl^- concentrations are present in sufficient excess for the rate to depend mainly on the concentration of NH_3. Harfmann and Crouch previously established that the Berthelot reaction is first order in respect of the NH_3 when OCl^- and phenol are in excess [35]. The linear region of the 60 min calibration was used to calculate a detection limit. This limit was found to be 27 μmol NH_3 L^{-1} at a signal-to-noise ratio of 3:1.

We examined the dependence of response on ionic strength. We used samples which were isotonic with serum and in which the salt concentration was 150 mmol NaCl L^{-1}. The rate and response was indistinguishable from the behavior of our sensor in 50 mmol BBS L^{-1}. These results confirm the sensing mechanism is not affected by high ionic strength and that the volume change is essentially independent of the ionic free energy of the system.

Sensor response to NH_3 in serum We also examined the response of our sensor to samples in diluted human blood serum. Serum is a more complex sensing medium than BBS because of the presence of salts, amino acids, and proteins. Although we seek to develop a sensor which works in whole blood, we are first testing our sensor in serum to avoid the errors associated with the generation of NH_3 in stored whole blood [10]. RBCs contain enzymes

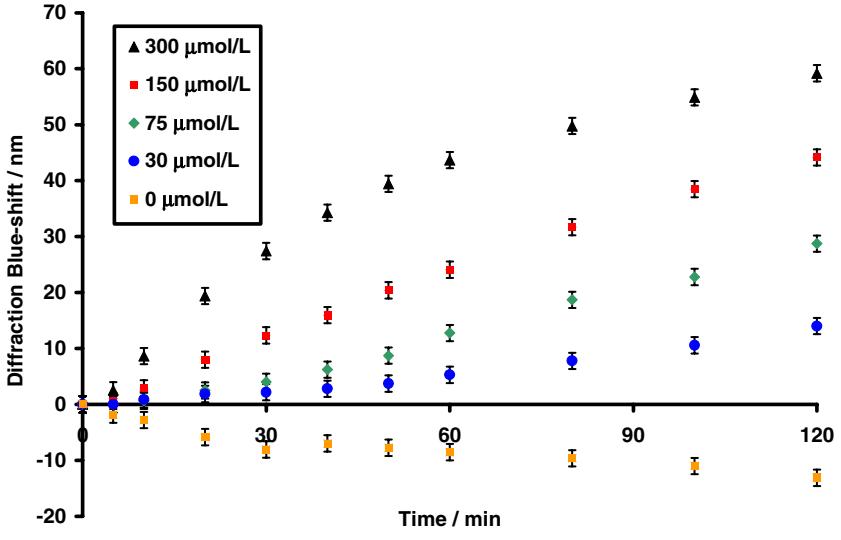

Fig. 5 Variation of diffraction blue-shift with time for ammonia-sensing PCCA in BBS at pH 9.2 containing 600 μmol OCl^- L^{-1}. The sensor has distinctly different rates of diffraction shift for different NH_3 concentrations; the control, containing no NH_3, actually red-shifts. The error bars are the average over the different time measurements of the standard deviation between replicate trials ($\lambda_{diffraction}$=±1.46 nm, N=3). The relative standard deviation remained fairly constant over time

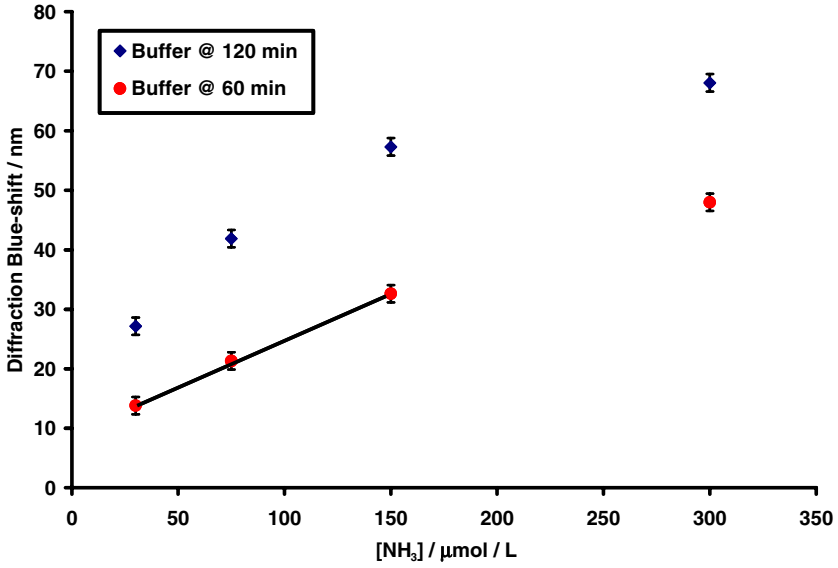

Fig. 6 Calibration plot based on the response of our sensor to NH_3 in BBS (pH=9.2) containing 600 µmol OCl^- L^{-1} at 60 and 120 min. This response of the sensor is linear between 30 and 150 µmol NH_3 L^{-1} at 60 min

that can increase the concentration of NH_3 with time after the blood is sampled. This rapidly raises the level of NH_3 in the samples to hyper-physiological levels.

Figure 7 shows the diffraction blue-shift as a function of time for four spiked serum samples (30, 75, 150, 300 µmol NH_3 L^{-1} spikes) and the normal, unspiked, sample.

Unlike the buffer, normal human serum contains a background level of NH_3. To determine the concentration of NH_3 in our unspiked sample, we used a Vitros 950 Chemistry System, the clinical instrument used by the University of Pittsburgh Medical Center. According to the Vitros determination, our normal serum solution had a background concentration of 4 µmol NH_3 L^{-1}.

The most remarkable difference between the sensor in buffer and in serum is the response to low NH_3 concentrations. In buffer without NH_3, the sensor responds to addition of OCl^- by red-shifting $\Delta\lambda$=14 nm. In the normal serum solution containing only 4 µmol NH_3 L^{-1}, the sensor responds to addition of OCl^- by blue-shifting $\Delta\lambda$=3 nm. We established that proteins were responsible for the blue-shift by analyzing an ammonia-free protein-rich solution of BSA (70 mg BSA mL^{-1} in BBS). The sensor also responded with a slight blue-shift ($\Delta\lambda$=3 nm) in the 2 h after OCl^- addition. We conclude the proteins in the serum are primarily responsible for the blue-shift in the unspiked serum.

Our observations correlate well with the description of Hawkins et al. [36, 37] of the reactivity of OCl^- towards proteins. They showed that OCl^- modifies the amino acid side-chains without significant degradation of the protein backbone at low OCl^- concentrations. Interactions of this type would result in reduction of the available OCl^- which would reduce the kinetics and extent of the reaction between OCl^- and NH_3. Although slow compared with the reaction with NH_3, the products of reactions between OCl^- and serum proteins could react further with the 3-AMP species on the hydrogel to cause the slight blue-shift observed.

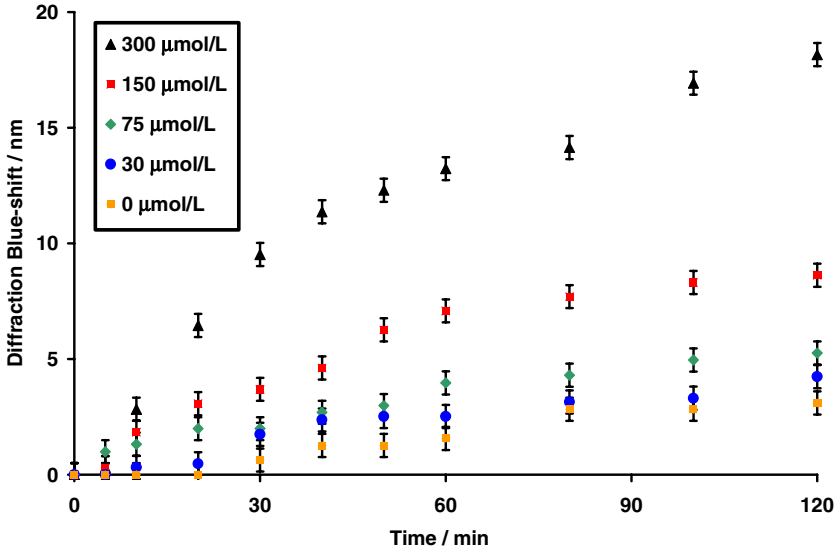

Fig. 7 We measured the PCCA response of four spiked serum samples and an unspiked sample. All samples contained 600 mmol OCl^- L^{-1} and had a pH of 9. We found the serum contained NH_3 at approximately the physiological concentration for healthy adults. The error bars are averages of the standard deviation for replicate trials ($\lambda_{diffraction}$=±0.57 nm, N=3)

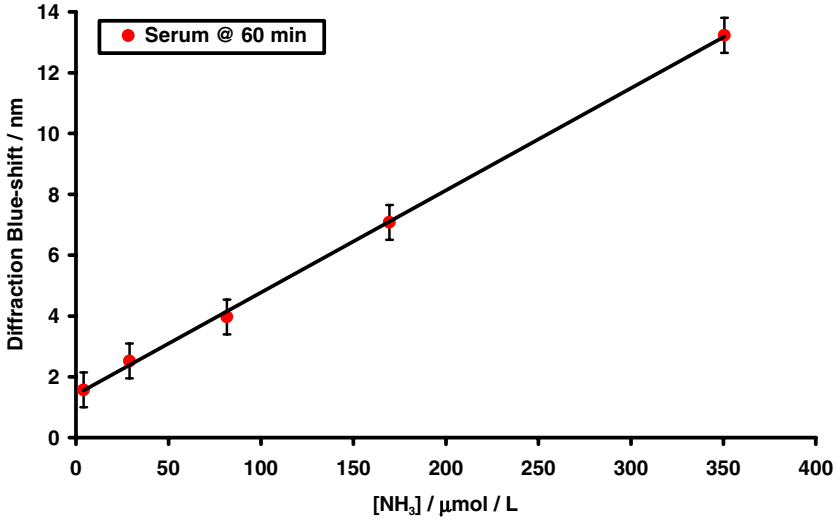

Fig. 8 Calibration plot for the response of our sensor to NH_3 in a 1:1 solution of serum and BBS at 60 min. Concentrations of NH_3 were determined using the Vitros Autoanalyzer. Error bars are equal to the standard deviation ($\lambda_{diffraction}$=±0.57 nm, N=3)

The diminished response observed in serum can be explained by previous studies, which report that the Berthelot reaction is subject to interference from proteins [18]. Ngo et al. [19] found that a solution containing 0.1 % human serum caused interference of 4 %. The manifestations of this interference are obvious for our sensor, because the response rate and the spectral window are both reduced by a factor of three in 50 % human serum solution. Despite this interference, we were able to establish a calibration plot for the spectral shift in response to the NH_3 concentration in serum. Figure 8 shows the calibration plot of the sensor's response to NH_3 at 60 min.

The response of the sensor is linear for concentrations of NH_3 between 0 and 350 µmol L^{-1}. We determined that the detection limit for our sensor was 50 µmol L^{-1} NH_3 at 60 min, and increases to 60 µmol L^{-1} NH_3 at 120 min. The detection limit was determined from three times the standard deviation of our control (λ=0.57 nm). The detection limit for the observed blue-shift (λ=3.12 nm) was used to calculate the [NH_3] detection limit use of linear regression. The increase in detection limit with time is because of the increase in the standard deviation of our spectral shifts at longer times and higher concentrations. The detection limit would also be increased at smaller times because the slope of the plot of response against concentration increases with time. The NH_3 present in the unspiked serum is below the detection limit of our sensor and cannot be distinguished from a serum sample containing no NH_3. Furthermore, the 30 µmol L^{-1} spiked sample cannot be distinguished from the unspiked sample at the >99 % confidence level. Table 1 (below) compares results from our sensor with those from current standard methods in clinical NH_3 sensing.

Table 1 Comparison of clinical reference interval and the operational interval of the PCCA and Vitros NH_3 methods

Clinical reference interval	10–300 µmol NH_3 L^{-1}
Ammonia-sensitive PCCA	50–350 µmol NH_3 L^{-1}
Vitros 950 Chemistry Autoanalyzer	1.0–500 µmol NH_3 L^{-1}

Future work and outlook

We are currently optimizing our reaction conditions, sample preparation, and hydrogel composition to improve sensitivity, spectral shift, and response time. We expect our technique could be modified to combine separation and detection into a single system by modification of the diffusion characteristics of our hydrogel or by using our material's thin-film morphology, which could be incorporated into a more complex sensing device. Separation of NH_3 from the sample would prevent interferences (RBCs, proteins, clotting, etc.) from affecting the sensor's performance.

The goal of our optimization is to develop a sensor responsive to NH_3 concentrations over the clinically relevant range with distinct visual color changes. Our sensor could then be used as a point-of-care device for the detection of blood NH_3 concentrations to monitor conditions arising from urea cycle disorders, organic acidemias, fatty acid oxidation defects, and hepatic disorders, to prevent patients from reaching hyperammonemic states. The ability to monitor these conditions at the bedside or at home with an inexpensive, robust system would provide long-term benefits both to patients and to health-care providers.

Conclusions

In the work described here we devised an NH_3-sensitive material in which we use the Berthelot reaction in our polymerized crystalline colloidal array (PCCA) sensing platform. Our material can be used for quantitative determination of NH_3 concentrations between 50 and 350 µmol NH_3 L^{-1} in human blood serum, which overlaps the clinically relevant range. The material responds to 300 µmol NH_3 L^{-1} additions with a spectral blue-shift of Δλ=60 nm in BBS and Δλ=20 nm in serum solution at 120 min. The detection limit is 27 µmol NH_3 L^{-1} in BBS

at 60 min and 50 μmol NH_3 L^{-1} in 50 % serum solution at 60 min with a confidence level of >99 %.

Acknowledgements We gratefully acknowledge NIH grants# 1 R01 GM 58821-01 and 2R01 DK 55348-03A1.

References

1. Huizenga JR, Gips CH, Tangerman A (1996) Ann Clin Biochem 33:23
2. Tietz NW (1995) Clinical laboratory guide to laboratory tests, 3rd edn. WB Saunders, Philadelphia
3. Pesce AJ, Kaplan LA (1987) Methods in clinical chemistry. CV Mosby Company, St. Louis
4. Hazell AS, Butterworth RF (1999) Exp Biol and Med 222:99
5. Campion M (2003) Blood ammonia: a critical measurement. BIMDG Bulletin Spring 13
6. Bachmann C (2003) Eur J of Pediatr 162:S29
7. Mondzac A, Ehrlich GE, Seegmiller JE (1965) J Lab Clin Med 66:526
8. Van Anken HC, Schiphorst ME (1974) A Clin Chim Acta 56:151
9. Vitros chemistry products AMON slides (2005) www.orthoclinical.com
10. Huizenga JR, Tangerman A, Gips CH (1994) Ann Clin Biochem 31:529
11. Mann LT (1963) Anal Chem 35:2179
12. Reay PF (1985) Anal Chim Acta 176:275
13. Lau KT, Edwards S, Diamond D (2004) Sens Actuators B 98:12
14. Daridon et al (2001) Sens Actuators B 76:235
15. Zellmer S, Katenborn G, Rothe U, Lehnich H, Lasch J, Pauer HD (1999) Anal Biochem 273:163
16. Berthelot M (1859) Rep Chim Appl I 284
17. Searle PL (1984) Analyst 109:549
18. Gips CH, Reitsema A (1971) Clin Chem Acta 33:257
19. Ngo TT, Phan APH, Yam CF, Lenhoff HM (1982) Anal Chem 54:46
20. Krieger IM, O'Neill FM (1968) J Am Chem Soc 90:3114
21. Hiltner PA, Krieger IM (1969) J Phys Chem 73:2386
22. Hiltner PA, Papir YS, Krieger IM (1971) J Phys Chem 75:1881
23. Carlson RJ, Asher SA (1984) Appl Spec 38:297
24. Runquist PA, Photinos P, Jagannathan S, Asher SA (1989) J Chem Phys 91:4932
25. Asher SA, Holtz JH, Liu L, Wu Z (1994) J Am Chem Soc 116:4997
26. Weissman JM, Sunkara HB, Tse AS, Asher SA (1996) Science 274:959
27. Ito K, Nakamura H, Ise N (1986) J Chem Phys 85:6136
28. Monovoukas Y, Gast AP (1989) J Colloid Interface Sci 128:533
29. Okubo T (1988) Acc Chem Res 21:281
30. Asher SA, U.S. Patents 4,627,689 (1986), 4,632,517 (1986), 5,281,370 (1994), 5,452,123 (1995)
31. Holtz JH, Asher SA (1997) Nature 389:829
32. Holtz JH, Holtz JS, Munro C, Asher SA (1998) Anal Chem 70:780
33. Pan G, Kesavamoorthy R, Asher SA (1998) J Am Chem Soc 120:6525
34. Goponenko AV, Asher SA J Am Chem Soc 127:10753
35. Harfmann RG, Crouch SR (1989) Talanta 36:261
36. Davies MJ (2005) Biochim Biophys Acta 1703:93
37. Hawkins CL, Pattison DI, Davies MJ (2003) Amino Acids 25:259